

Spatial dispersion in CaF_2 caused by the vicinity of an excitonic bound state.

M. Letz^a, W. Mannstadt^a, M. Brinkmann^a, and E. Mörsen^b

^a Schott Glas, Research and Development, D-55014 Mainz, German y and

^b Schott Lithotec AG, Otto-Schott Str. 13, D-07705 Jena, Germany

The microscopic mechanism beyond the optical anisotropy of an ionic crystal which occurs for short wavelengths is investigated. The electron-hole, two particle propagator and its analytical behaviour close to the band edge of the one particle continuum plays a major role for the mechanism of this optical anisotropy. Especially for an ionic crystal the two particle bound state, the exciton, is of special importance. In this way we argue that the so called “intrinsic birefringence” in CaF_2 is neither intrinsic to the material nor it is birefringence. Instead it is spatial dispersion caused by the vicinity of a dispersive optical absorption given by the excitonic bound state. We propose a model which connects the bound state dispersion with the band structure and a model potential for a screened coulomb interaction. Based on these considerations we predict a wavelength dependence of the dielectric function approaching close to the bound state level $\epsilon \sim (\lambda - \lambda_0)^{-1}$, where λ_0 is the wavelength of the excitonic bound state level.

PACS numbers:

I. INTRODUCTION

There is no doubt that CaF_2 is the key component for establishing 157nm UV lithography. Its perfect cubic symmetry together with a great homogeneity of large single crystals which are very stable under normal conditions makes it a perfect material for homogeneous optical lens design.

However, there is a severe shortcoming of the material on which the attention was focused within the last year. This is the so called “intrinsic birefringence”.¹ For the first glance it is astonishing. Looking at standard textbooks (e.g.²) we note that a cubic crystal does not show any birefringence. On the other hand experiments observe a spatial dependence of the dielectric properties. Light propagating along different directions through the crystal shows a deviation between different polarization directions which is of the order of 10^{-6} nm/cm for UV light with 157nm. Or with other words the dielectric function depends on the direction in which the light propagates through the crystal and shows a difference which is of the order of 10^{-6} .

How can this obvious misfit between standard textbooks and recent observations in CaF_2 be resolved? The answer leads back to a physical phenomenon which is known as spatial dispersion.³

The statement “a cubic system does never show birefringence” can be proven exactly, since in a cubic system the ellipsoid corresponding to the dielectric function is always a sphere. The question remains: What is a “system”? The crystal of CaF_2 has exactly cubic symmetry but the “system” of light interacting with this perfectly cubic crystal shows a deviation from cubic symmetry. This is due to the fact that the light carries a \mathbf{q} vector pointing in the vacuum in the direction of propagation. This is a consideration which has been already made more than one century ago⁴. However the speed of light is much larger than any speed in a solid state system and therefore one can usually safely neglect the

wave-vector dependence of the propagating light. This statement is identical to the wavelength of light being in the optical window much larger than any length scale in a solid.

There are however two important exceptions where the assumption made above ceases to be valid. The first (I) is when one is by far leaving the optical window. This is the case at X-ray scattering experiments. Here the wavelength of light is of the order of the lattice constant and this causes a wave-vector (spatial) dependence of the resulting scattering signal. The second case (II) which is valid for CaF_2 and many other solids is the case of light in the vicinity of a dispersive absorption occurring also at small wavevectors (large length scales). Since the dielectric function is an analytic function it has to follow causality which is expressed in the Kramers-Kronig relation between its real and imaginary part. The vicinity of a band edge can cause spatial dispersion in a semiconductor system (see e.g.⁵).

In a semiconductor, the absorption is mainly dominated by the band edge and an exciton, the two particle bound state of the electron-hole pair only plays a minor role. The situation changes if we look at ionic crystals like CaF_2 . Here screening of the bare coulomb interaction is less effective which expresses itself in deep excitonic bound states. This is expressed in the exciton intensity being inverse proportional to the third power of the static dielectric function $I \sim \epsilon_0^{-3}$.⁶ The connection between a dispersive excitonic bound state and spatial dispersion has been already discussed for KI.⁷

When discussing possible alternative material designs to CaF_2 it is important to understand the microscopic mechanism beyond the spatial dispersion in great detail and it is in particular important to know and predict the exciton dispersion.

The paper is organized as follows: In section II we define the system in the case when the approximation of locality breaks down. In section III we review the connection between the electronic part of the dielectric

function and the bare two-particle propagator. We look at the free two particle propagator in the absence of any screened coulomb attraction and its connection to the band structure. The connection between the band structure, which can e.g. be based on DFT (density functional theory) calculations, and the dynamic polarization is investigated in section IV. In the following (section V) we discuss analyticity based on the resulting pole structure of the dielectric function. This describes to a large part the situation in a semiconductor where no deep bound state is present. Section (VI) serves to introduce the two body problem of the electron hole pair which leads to the excitonic bound state when a reasonable assumption for the weakly screened coulomb attraction has been made. Based on the model assumptions made, we discuss the spatial dispersion of CaF_2 close to the bound state level in section VII and compare our predictions with the experimental work of.¹

II. SYSTEM OF CaF_2 INTERACTING WITH LIGHT

Light has a \mathbf{q} vector pointing along its propagation direction. This wave-vector becomes important when the light is interacting with a long wavelength ($\mathbf{q} \rightarrow 0$) excitation of the system. In an isotropic medium this wave vector dependence will only depend on the absolute value of \mathbf{q} . In liquids and glasses this leads e.g. to the observation of hydrodynamic modes (phonon modes) in light scattering experiments.⁸ In single crystals the situation is different as not only the dependence on the absolute value of the wavevector of the light is important but also the direction of the wave vector with respect to the crystal orientations. The crystal of CaF_2 possesses ideal cubic symmetry. That means in the static limit that also all response functions have to show this symmetry. Dynamically there are situations especially close to a strong excitation at long wavelengths, when the breaking of cubic symmetry due to the incident light gets important. Therefore not only the dynamic of a dielectric response has to be considered but also the wave-vector dependence. The electric field \mathbf{E} is connected with the electric induction \mathbf{D} in a non-local way.

$$\mathbf{D}(\mathbf{q}, \omega) = \epsilon(\mathbf{q}, \omega) \mathbf{E}(\mathbf{q}, \omega) \quad (1)$$

where $\epsilon(\mathbf{q}, \omega)$ is the dynamic dielectric function. For the physics of the spatial dispersion in CaF_2 we will focus on the part of the dynamic dielectric function which is caused by electronic excitations. In general the dielectric function is an analytic function defined on the complex ω -plane. Along the real axis it has a real and imaginary part.

$$\epsilon(\mathbf{q}, \omega) = \epsilon'(\mathbf{q}, \omega) + i\epsilon''(\mathbf{q}, \omega) \quad (2)$$

Only in the static limit $\omega \rightarrow 0$ one can assign a physical value to the real and imaginary part separately. The real

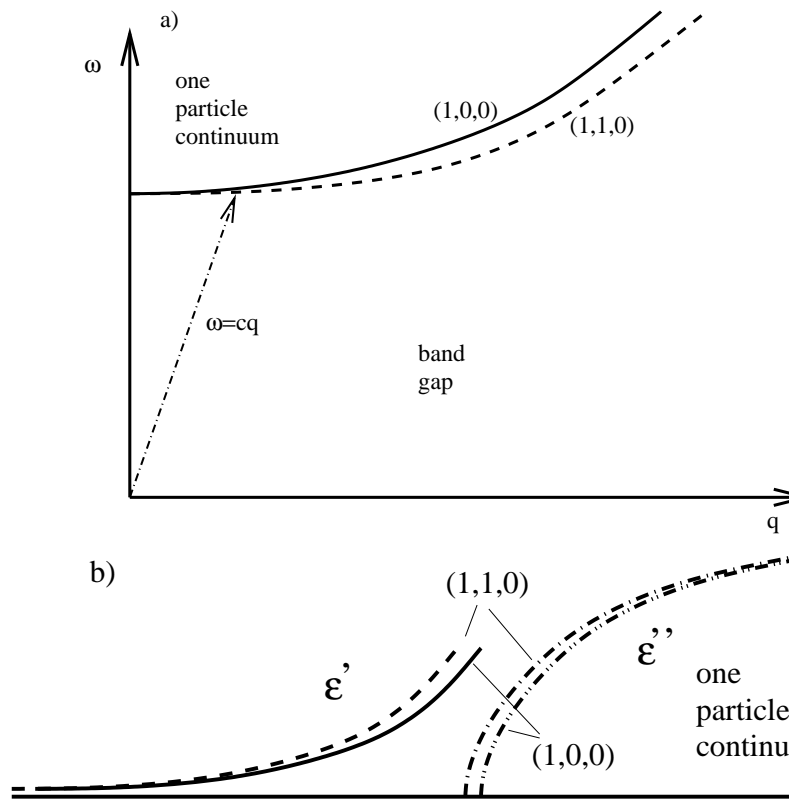


FIG. 1: Schematic plot of the pole structure of the two particle correlation function $\Pi^0(\mathbf{q}, \omega)$ as it can occur for different directions of the wave vector. $\Pi^0(\mathbf{q}, \omega)$ is in the case when no excitonic bound state exists proportional to the dielectric function. In Fig. a) we have plotted the band gap. The band gap can have a different shape when looking along different \mathbf{q} directions. Above the band gap the two particle continuum starts where there is always a non zero imaginary part of the dielectric function. The light dispersion $\omega = cq$ is plotted schematically. In Fig. b) the real and imaginary part of the dielectric function resulting from Kramers-Kronig relations are plotted in a schematic way. When approaching the band gap the real part of the dielectric function bends up (but will not diverge in a 3D system) and the imaginary part will show a $\sqrt{\omega - \omega_0}$ behaviour.

part is connected with polarizabilities and the imaginary part with mobile charges ($\epsilon''(\omega) = \lim_{\omega \rightarrow 0} 4\pi\sigma(\omega)/\omega$) which are absent in an insulator. For a general crystal the dielectric function is a tensor. Since we want to keep the equations as transparent as possible we do not write tensor indices. We assume a coordinate system placed along the main axes of the cubic crystal. For a cubic crystal like CaF_2 we can concentrate on specific directions of the \mathbf{q} vector. Symmetry considerations allow to decompose all tensorial quantities into its symmetry components. This will provide rules to fill all the components of the tensorial dielectric function.

III. THE DYNAMIC DIELECTRIC FUNCTION

The optical frequency regime is above the infrared optical phonon modes and below excitations over the band gap. In this regime the dynamical dielectric function can be decomposed in two parts.

$$\epsilon(\mathbf{q}, \omega) = \epsilon_\infty + \epsilon_{e^- - h^+}(\mathbf{q}, \omega) \quad (3)$$

Where ϵ_∞ is the IR-dielectric function which in a cubic crystal like CaF_2 will be not only real but completely isotropic. The subscript ∞ refers to frequencies above the IR optical phonon modes but is still far below excitations over the bandgap. Wave-vector dependence only enters from the second part which stems from electron hole excitations. The electron-hole dielectric function is proportional to the proper electron-hole polarization propagator⁹

$$\epsilon_{e^- - h^+}(\mathbf{q}, \omega) \sim \Pi^*(\mathbf{q}, \omega) \quad (4)$$

Where $\Pi^*(\mathbf{q}, \omega)$ is the propagator of an electron hole pair with total momentum \mathbf{q} . In the following we do not want to focus on details but rather want to outline the pole structure of this two particle propagator since it gives further insight into the problem.

IV. CONNECTION TO THE BAND STRUCTURE

If we look for the first glance at the bare electron hole propagator $\Pi^0(\mathbf{q}, \omega)$ we can make the connection to the band structure.

$$\Pi^0(\mathbf{q}, \omega) = \frac{1}{N} \sum_{\mathbf{k}} \frac{f(\mathbf{k}, \mathbf{q}, \omega)}{\omega - (E^{e^-}(\mathbf{k} + \mathbf{q}) - E^{h^+}(\mathbf{k}))} \quad (5)$$

The detailed form of the numerator can be taken from textbooks⁹ while the pole structure is connected with the electronic band structure. In general Eq. (5) should also contain a sum over all bands. Since we are approaching the band gap from the low frequency site and we know that CaF_2 has a direct band gap we are for a first glance only interested in the highest valence band $E^{h^+}(\mathbf{k})$ and the lowest conduction band $E^{e^-}(\mathbf{k})$ around the Γ point at $\mathbf{k} = (0, 0, 0)$. Even in a cubic crystal the band structure will show a different \mathbf{k} dependence when looking along different directions in the crystal. In particular the $(1, 0, 0)$ direction will differ from the $(1, 1, 0)$ and $(1, 1, 1)$ direction.

V. ANALYTIC PROPERTIES OF THE DIELECTRIC FUNCTION

From the analyticity of $\Pi^0(\mathbf{q}, \omega)$ we can derive the qualitative behaviour of its real and imaginary part. This

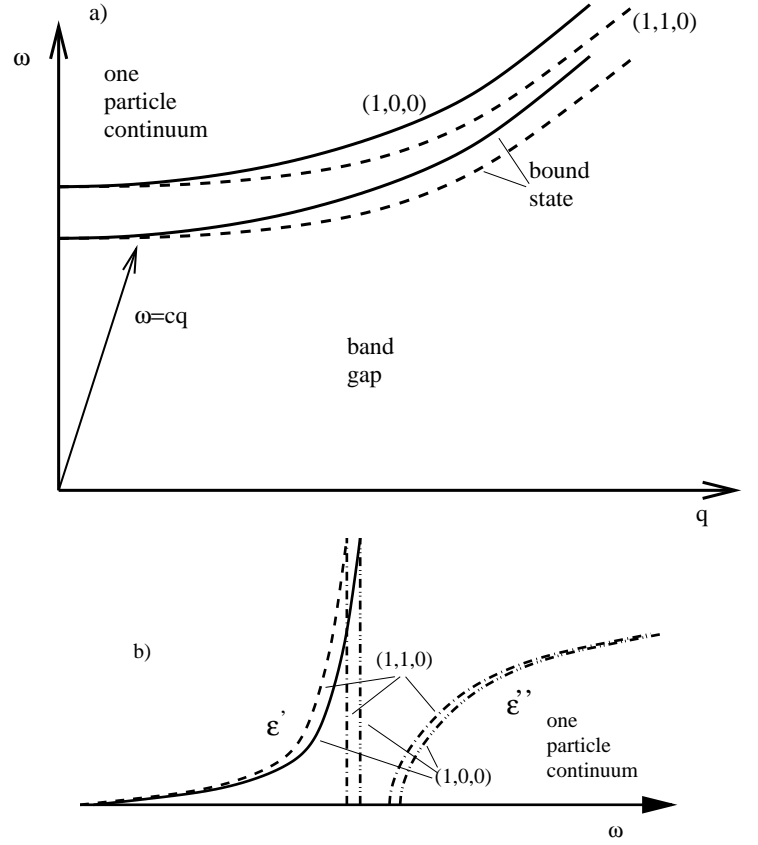


FIG. 2: Schematic plot of the pole structure proper polarization $\Pi^*(\mathbf{q}, \omega)$ (proportional to $\epsilon_{e^- - h^+}(\mathbf{q}, \omega)$) as it can occur for different directions of the wave vector in an ionic crystal where a strong excitonic bound state is present. In Fig. a) we have plotted the band gap. The band gap can have a different shape when looking along different \mathbf{q} directions. Above the band gap the two particle continuum starts where there is always a non zero imaginary part of the dielectric function. The bound state can occur below the one particle continuum. For simplicity we have only plotted the ground state level of only one exciton. The light dispersion $\omega = cq$ is plotted schematically. In Fig. b) the real and imaginary part of the dielectric function resulting from Kramers-Kronig relations are plotted in a schematic way. When approaching the bound state the real part of the dielectric function diverges as $(\omega - \omega_0)^{-1}$ where ω_0 is the bound state level.

is plotted schematically in Fig. 1. In Fig. 1a the structure is shown in the $\omega - q$ plane. There is the large band gap. An excitation over the bandgap is the creation of an electron-hole pair. Above the band gap there is a continuum of one particle excitations. The light dispersion is shown as well. Since the speed of light is much larger than any electronic speed one can usually in the optical frequency range safely neglect the wave-vector dependence of the light and use $\mathbf{q} = 0$. This breaks down when excitations are considered which come close to the band gap. In this case it can become important that the band curvature is different along different directions in the crystal. Schematically we have plotted here a fictitious $(1, 1, 0)$ and $(1, 0, 0)$ band curvature.

In Fig. 1b the resulting real and imaginary part of $\Pi^0(\mathbf{q}, \omega)$ is plotted resulting from the Kramers-Kronig

relations. In a three dimensional system the imaginary part of the one particle continuum shows a $\sqrt{\omega - \omega_0}$ behaviour. Therefore the real part does not diverge at the band edge (opposite to a 1D or 2D system) but increases up to a finite value. In order to keep the plots in Fig. 1 as simple as possible we have not plotted the real part of the polarizability above the gap.

If for different wave-vector directions in the crystal the band gap is shifted one can observe a spatial dispersion. This is the case in semiconductors where no deep excitonic bound state exists.⁵ Here the spatial dispersion is caused by the wave-vector dependence of the one particle continuum. A weak attractive electron-hole interaction will not change the picture as long as no strong excitonic bound states are created below the one particle continuum. Therefore in these cases the dielectric function can already be described using $\epsilon \sim \Pi_0$. The situation is completely different in a strongly ionic crystal like CaF_2 here the excitonic bound state becomes important.

VI. THE TWO PARTICLE BOUND STATE OF THE EXCITON

In a strongly ionic crystal screening is less effective and the coulomb attraction between the positively charged hole and the negatively charged electron leads to the formation of a strong two particle bound state. The solution of this two body problem involves in general a solution of the Bethe-Salpeter equation (see e.g.¹⁰). However the basic principal of this bound state formation can already be understood with a much simpler interaction. The full solution for a complicated electron hole interaction for CaF_2 has been taken into account in¹¹ here we just want to highlight the basic principles under which such a solution leads to an excitonic bound state. When we assume the attractive interaction to be only a function of the total momentum of the electron-hole pair $U(\mathbf{q})$, the equations can be solved easily and one gets a RPA (random phase approximation) denominator for the proper polarization which stems from a summation of a geometrical series.

$$\Pi^*(\mathbf{q}, \omega) = \frac{\Pi^0(\mathbf{q}, \omega)}{1 - U(\mathbf{q}) \Pi^0(\mathbf{q}, \omega)} \quad (6)$$

This is also known as the ladder approximation to the Bethe-Salpeter equation. New physics will occur when the denominator of Eq. (6) shows additional poles beside the one particle continuum. This is the case when the denominator of Eq. (6) gets zero.

$$1 - U(\mathbf{q}) \Pi^0(\mathbf{q}, \omega) = 0 \quad (7)$$

If this happens outside the one particle continuum a true bound state, the exciton is formed. Finding the bound state level can be schematically seen in Fig. 1b. When drawing a line at $f(\omega) = 1/U(\mathbf{q})$ it can for large U , for large attractive interactions cross the real part of

Π^0 . This crossing marks the bound state level where a new pole occurs. Such a situation with a bound state is schematically sketched in Fig. 2. Below the one particle continuum the exciton level occurs as a true pole. The dynamic polarization and therefore also the dielectric function has to follow Kramers-Kronig relations connecting its real and imaginary part. In the vicinity of a true pole the real part of the dielectric function has to follow the asymptotic behaviour as

$$\epsilon'_{e-h+}(\mathbf{q}, \omega) \sim \Re(\Pi^*(\mathbf{q}, \omega)) \sim \frac{1}{\omega - \omega_{ex}(\mathbf{q})} = \frac{2\pi c}{\frac{1}{\lambda} - \frac{1}{\lambda_{ex}(\mathbf{q})}} = \frac{2\pi c \lambda \lambda_{ex}}{\lambda_{ex}(\mathbf{q})} \quad (8)$$

The wave-vector dependence of the exciton level $\omega_{ex}(\mathbf{q})$ (or $\lambda_{ex}(\mathbf{q})$) will in general differ along different directions in the crystal. This is schematically plotted in Fig. 2a. Exactly this difference causes the spatial dispersion seen in ionic crystals like CaF_2 and BaF_2 .

VII. SPATIAL DISPERSION IN CaF_2 AND PREDICTIONS FOR EXPERIMENTAL OBSERVATIONS

In view of the measurements performed by Burnett et al.¹ we need the refractive index along different directions. In an isotropic medium this is where the dielectric function is diagonal with three identical diagonal elements this would be simply given by:

$$n(\omega) = \sqrt{\epsilon(\omega)} \quad (9)$$

with ϵ being the (real part of the) diagonal part of the diagonalized dielectric function.

The concept of a refractive index becomes by far more sophisticated as soon as the medium shows anisotropies. This is also the case for CaF_2 . Here one has to go into a new coordinate system whose z-direction is determined by the \mathbf{q} -direction of the incident light. Two possible directions perpendicular to the z-direction complete this new coordinate system and are denoted with Greek letters α, β . Within the α - β -plane lies the polarization vector \mathbf{e} pointing in the direction of the electric induction \mathbf{D} of the light. Within this new coordinate system the calculation of the refractive index is given by the zero of a two dimensional determinant.³

$$\text{Det} \begin{vmatrix} n^{-2} \delta_{\alpha, \beta} - \epsilon_{\alpha, \beta}^{-1}(\mathbf{q}, \omega) \end{vmatrix} = 0 \quad (10)$$

In general the eigenvalue problem of Eq. (10) has two solutions which correspond to the main polarization axes.

There is a further difference to an anisotropic medium. This is the fact that the wave-vector \mathbf{q} is not in general parallel to the Poynting-vector \mathbf{S} which points along the direction of the group velocity which is the analogon of the path in classical geometrical optic. This is expected to be small in a cubic crystal.

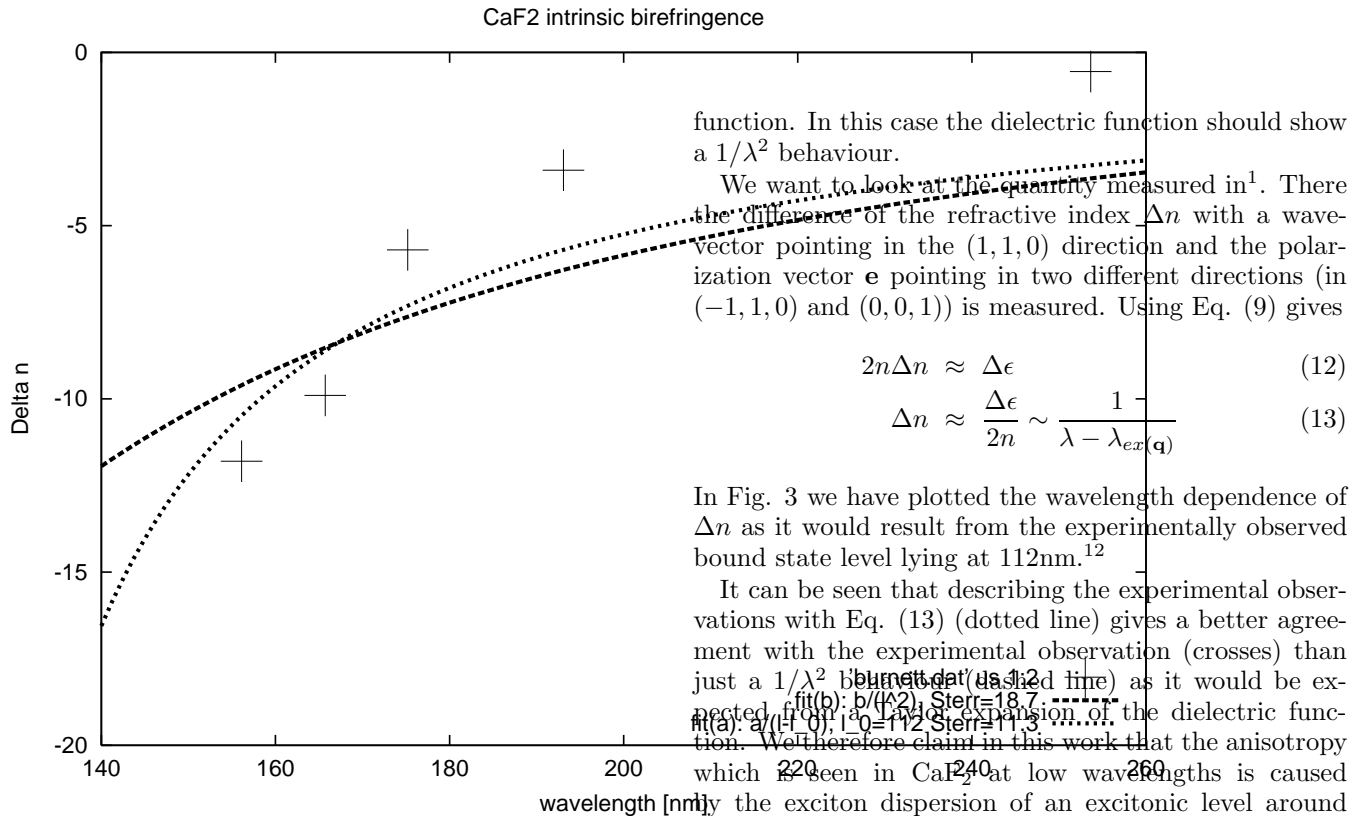


FIG. 3: Comparison of the data from¹ (crosses) with a $1/\lambda^2$ (dashed line) and a $1/(\lambda - \lambda_{ex}(\mathbf{q}))$ (dotted line) behaviour. The $1/\lambda^2$ behaviour results from a Taylor expansion of the dielectric function (dashed line). A comparison with the function which results from the vicinity of a dispersive bound state (exciton) is plotted (dotted line). For the exciton wavelength the 112nm known from literature¹² were used. The exciton model produces a better description of the data at smaller wavelength. It further makes the prediction that the dielectric properties will for wavelength below 157nm diverge as $1/(\lambda - \lambda_{ex}(\mathbf{q}))$ when approaching the excitonic bound state.

So the refractive index is dependent on \mathbf{q} and can for a given experimental setup be dependent on the polarization direction of the incident light.

$$n = n(\mathbf{q}, \omega) = n(\mathbf{q}, 2\pi c/\lambda) \quad (11)$$

In a cubic crystal like CaF_2 there are several exceptions for the wave-vector \mathbf{q} and the Poynting vector pointing along the same direction where no dependence on the polarization direction occurs as one can derive from symmetry considerations. One is for example light propagating along the main axis of the crystal (e.g. $\mathbf{q} = (1, 0, 0)$ now measured in the coordinate system of the crystal axes).

The dielectric function diverges close to the excitonic bound state depending on the wave-vector \mathbf{q} according to Eq. (8) with $\lambda_{ex}(\mathbf{q})$ is the wavelength of the exciton for the given \mathbf{q} vector. This wavelength must be for CaF_2 close to the 112nm where the exciton is found experimentally¹².

Note that Eq. (8) is quite different to what would result from just a formal Taylor expansion of the dielectric

function. In this case the dielectric function should show a $1/\lambda^2$ behaviour.

We want to look at the quantity measured in¹. There the difference of the refractive index Δn with a wave-vector pointing in the (1,1,0) direction and the polarization vector \mathbf{e} pointing in two different directions (in $(-1, 1, 0)$ and $(0, 0, 1)$) is measured. Using Eq. (9) gives

$$2n\Delta n \approx \Delta\epsilon \quad (12)$$

$$\Delta n \approx \frac{\Delta\epsilon}{2n} \sim \frac{1}{\lambda - \lambda_{ex}(\mathbf{q})} \quad (13)$$

In Fig. 3 we have plotted the wavelength dependence of Δn as it would result from the experimentally observed bound state level lying at 112nm.¹²

It can be seen that describing the experimental observations with Eq. (13) (dotted line) gives a better agreement with the experimental observation (crosses) than just a $1/\lambda^2$ behaviour (dashed line) as it would be expected from a Taylor expansion of the dielectric function. We therefore claim in this work that the anisotropy which is seen in CaF_2 at low wavelengths is caused by the exciton dispersion of an excitonic level around 112nm (11.2eV). Especially measurements in the wavelength range between 112nm and 157nm we predict to show a clear $1/(\lambda - \lambda_{ex}(\mathbf{q}))$ behaviour.

VIII. CONCLUSION

We argue that the optical anisotropy observed in CaF_2 is caused by exciton dispersion. The delocalized exciton lies at approximately 112nm. Using this excitonic model the measured data on the optical anisotropy can be well explained and it is predicted that the dielectric function should diverge for lower wavelengths as $1/(\lambda - \lambda_{ex}(\mathbf{q}))$. Here $\lambda_{ex}(\mathbf{q})$ is the wavelength of the excitonic bound state.

If the connection to the exciton is indeed the dominant mechanism beyond the optical anisotropy all possible compensation approaches have to be reviewed. E.g. forming solid solution crystals, if possible at all, would only lead to an improvement, if the exciton dispersion will be smaller in such a crystal. Further the subtle difference between the spatial dispersion and birefringence has to be taken into account in a very careful way when performing lens design.

Acknowledgments

M.L. thanks D.Strauch and K.Schmalzl for helpful discussions and for band structure data on CaF_2 . The work was supported by the BMBF project ‘‘Laserbasierte Ultrapräzisionstechnik – 157nm Lithographie, Teilvorhaben: Optische Materialien und Komponenten für die 157nm Lithographie, AP 4210’’.

-
- ¹ J.H. Burnett, Z.H. Levine, E.L. Shirley, "Intrinsic birefringence in calcium fluoride and barium fluoride," *Phys. Rev. B* **64** 241102R, (2001).
- ² J. Nye, *Physical properties of crystals*, pp. 237, Oxford University Press, Oxford, (1979).
- ³ L.D. Landau, E.M. Lifshitz, *Elektrodynamik der Kontinua*, pp. 455, Akademie Verlag, Berlin, (1985).
- ⁴ H.A. Lorentz, "Collected papers (martinus nijhoff, the hague)," Vol. II p.79, Vol III, p. 314, (1936).
- ⁵ P.Y. Yu, M. Cardona, "Spatial dispersion in the dielectric constant of gaas," *Sol. Stat. Com* **9**, 1421, (1971).
- ⁶ J.C. Philips, "Ionicity of the chemical bond in crystals," *Rev. Mod. Phys.* **42**(3), 317, (1970).
- ⁷ F. Meseguer, M. Cardona, A. Cintas *Sol. Stat. Com.* **50**, 371, (1984).
- ⁸ A. Latz, M. Letz, "On the theory of light scattering in molecular liquids," *Eur. Phys. J. B* **19**, 323, 2001.
- ⁹ A.L. Fetter, J.D. Walecka, "*Quantum theory of many particle systems*", pp. 151, McGraw Hill, San Francisco, (1971).
- ¹⁰ M. Rohlfing, S.G. Louie, "Excitonic effects and the optical absorption spectrum of hydrogenated si clusters," *Phys. Rev. Lett.* **80**(15), 3320, (1998).
- ¹¹ L.X. Benedict, E.L. Shirley, "Abinitio calculation of $\epsilon_2(\omega)$ including the electron-hole interaction: Application to GaN and CaF₂," *Phys. Rev. B* **59**, 5441, (1999).
- ¹² T. Tomiki, T. Miyata, "Optical studies of alkali fluorides and alkaline earth fluorides in vuv region," *J. Phys. Soc. Jpn* **27**, 658, (1969).